JB
Journals.ASM.org

Novel, Highly Specific *N*-Demethylases Enable Bacteria To Live on Caffeine and Related Purine Alkaloids

Ryan M. Summers,[a,b] Tai Man Louie,[a,b] Chi-Li Yu,[a,b] Lokesh Gakhar,[c] Kailin C. Louie,[a] and Mani Subramanian[a,b]

Department of Chemical and Biochemical Engineering, University of Iowa, Iowa City, Iowa, USA[a]; The Center for Biocatalysis and Bioprocessing, University of Iowa, Coralville, Iowa, USA[b]; and Protein Crystallography Facility, University of Iowa, Iowa City, Iowa, USA[c]

The molecular basis for the ability of bacteria to live on caffeine as a sole carbon and nitrogen source is unknown. *Pseudomonas putida* CBB5, which grows on several purine alkaloids, metabolizes caffeine and related methylxanthines via sequential *N*-demethylation to xanthine. Metabolism of caffeine by CBB5 was previously attributed to one broad-specificity methylxanthine *N*-demethylase composed of two subunits, NdmA and NdmB. Here, we report that NdmA and NdmB are actually two independent Rieske nonheme iron monooxygenases with N_1- and N_3-specific *N*-demethylation activity, respectively. Activity for both enzymes is dependent on electron transfer from NADH via a redox-center-dense Rieske reductase, NdmD. NdmD itself is a novel protein with one Rieske [2Fe-2S] cluster, one plant-type [2Fe-2S] cluster, and one flavin mononucleotide (FMN) per enzyme. All *ndm* genes are located in a 13.2-kb genomic DNA fragment which also contained a formaldehyde dehydrogenase. *ndmA*, *ndmB*, and *ndmD* were cloned as His_6 fusion genes, expressed in *Escherichia coli*, and purified using a Ni-NTA column. NdmA-His_6 plus His_6-NdmD catalyzed N_1-demethylation of caffeine, theophylline, paraxanthine, and 1-methylxanthine to theobromine, 3-methylxanthine, 7-methylxanthine, and xanthine, respectively. NdmB-His_6 plus His_6-NdmD catalyzed N_3-demethylation of theobromine, 3-methylxanthine, caffeine, and theophylline to 7-methylxanthine, xanthine, paraxanthine, and 1-methylxanthine, respectively. One formaldehyde was produced from each methyl group removed. Activity of an N_7-specific *N*-demethylase, NdmC, has been confirmed biochemically. This is the first report of bacterial *N*-demethylase genes that enable bacteria to live on caffeine. These genes represent a new class of Rieske oxygenases and have the potential to produce biofuels, animal feed, and pharmaceuticals from coffee and tea waste.

Many natural products and xenobiotic compounds contain *N*-linked methyl groups. A search of the Combined Chemical Dictionary database (http://ccd.chemnetbase.com) identified 19,091 compounds out of approximately 500,000 entries that contain at least one *N*-methyl group. *N*-Demethylations of many of these compounds by members of cytochrome P450, flavoenzyme, and 2-ketoglutarate-dependent nonheme iron oxygenase families are critical biological processes in living organisms (1, 12, 17, 27, 31). These processes include detoxification of drugs and xenobiotic compounds, regulation of chromatin dynamics and gene transcription, and repair of alkylation damages in purine and pyrimidine bases in nucleic acids. Members of all aforementioned enzyme families also catalyze *O*-demethylation reactions (14). Bacteria have evolved highly specific Rieske [2Fe-2S] domain-containing *O*-demethylases that belong to the Rieske oxygenase (RO) family for the degradation of methoxybenzoates (5, 16). However, to the best of our knowledge, there is no description of *N*-demethylation by ROs.

Caffeine (1,3,7-trimethylxanthine) and related *N*-methylated xanthines are purine alkaloids that are extensively used as psychoactive substances and food ingredients by humans. Humans metabolize caffeine mainly via *N*-demethylation catalyzed by the hepatic cytochrome P450s 1A2 and 2E1 (2). Various bacteria have been reported to metabolize caffeine and related methylxanthines by *N*-demethylation. However, nothing is known about the genes involved (8), although this topic has recently attracted popular press (http://www.uiowa.edu/~biocat/datafiles/CBB5/CBB5%20Articles.pdf). The nature of bacterial *N*-demethylases has remained elusive, since they have been reported as unstable in conventional purification procedures (8). We recently isolated a caffeine-degrading bacterium, *Pseudomonas putida* CBB5, from soil by enrichment on caffeine as the sole source of carbon and nitrogen (34). CBB5 is unique because it completely *N*-demethylates caffeine and all related methylxanthines, including theophylline (1,3-dimethylxanthine), which is rarely metabolized by bacteria, to xanthine.

A novel methylxanthine *N*-demethylase (Ndm) with broad substrate specificity was purified from CBB5 (30). Ndm was characterized as a soluble oxygenase composed of two subunits, NdmA and NdmB, with apparent molecular masses of 40 and 35 kDa, respectively. The *N*-demethylation activity of Ndm was dependent on a specific reductase present in CBB5, which oxidized NAD(P)H and presumably transferred electrons to Ndm for *N*-demethylation. Ndm was hypothesized to be an RO based on its reductase dependence, stimulation of activity by exogenous Fe^{2+}, UV/visible absorption spectrum, utilization of oxygen as a cosubstrate, and homology of the N-terminal amino acid sequences of NdmA and NdmB to those of two hypothetical ROs. The oxygenase components of all crystallized ROs are either in α_3 or $\alpha_3\beta_3$ configurations, with the α subunit serving as the catalytic subunit and the β subunit serving a structural purpose (11). Molecular masses of the α and β subunits are typically 40 to 50 kDa and 20

Received 2 December 2011 **Accepted** 1 February 2012
Published ahead of print 10 February 2012
Address correspondence to Mani Subramanian, mani-subramanian@uiowa.edu.
R.M.S. and T.M.L. contributed equally to this work.
Supplemental material for this article may be found at http://jb.asm.org/.

doi:10.1128/JB.06637-11

kDa, respectively. The fact that both NdmA and NdmB, inseparable by several chromatographic steps, are similar in size to the α subunits of ROs led us to hypothesize that they could be individual *N*-demethylating ROs with different properties that copurified from CBB5. Here, we report cloning of a 13.2-kb gene cluster from CBB5. Genes encoding NdmA, NdmB, and the reductase (NdmD) were identified within this gene cluster. Functional expression of these genes in *Escherichia coli* and biochemical characterization of the recombinant enzymes substantiated NdmA and NdmB as individual ROs with highly specific N_1- and N_3-demethylation activities, respectively, on methylxanthines. NdmD was absolutely required for the activities of NdmA and NdmB.

MATERIALS AND METHODS

Chemicals. Caffeine, theophylline, theobromine, paraxanthine, 1-methylxanthine, 3-methylxanthine, 7-methylxanthine, xanthine, ammonium acetate, acetic acid, 2,4-pentanedione, and bovine cytochrome *c* were purchased from Sigma-Aldrich (St. Louis, MO). Tryptone, yeast extract, Soytone, and agar were obtained from Becton Dickinson and Company (Sparks, MD). NADH, isopropyl β-D-thiogalactopyranoside (IPTG), 5-bromo-4-chloro-3-indolyl β-D-galactopyranoside (X-Gal), and Tris base were obtained from RPI Corp. (Mt. Prospect, IL). Restriction enzymes were purchased from New England BioLabs (Ipswich, MA). *Pfu*Ultra DNA polymerase (Stratagene, Santa Clara, CA), *Taq* DNA polymerase, and Phusion HF polymerase (both from New England BioLabs) were used in various PCRs as indicated. PCR primers were purchased from Integrated DNA Technologies (Coralville, IA). High-pressure liquid chromatography (HPLC)-grade methanol (J.T. Baker, Phillipsburg, NJ) was used in all chromatographic studies.

PCR amplification of *ndmA*- and *ndmB*-containing genomic DNA fragments plus flanking regions from the CBB5 genome. The procedures used to create two genomic DNA libraries and generate eight overlapping PCR fragments that spanned 13.2 kb of CBB5 genome are reported in detail in the supplemental material. Analyses of open reading frames (ORFs) were performed manually with the help of GeneMark.hmm for prokaryotes (23), FGENSB (Softberry, Inc., Mount Kisco, NY), and GLIMMER (9).

Cloning and heterologous expression of *ndmA*, *ndmB*, and *ndmD*. Forward primer pET-ndmA-F and reverse primer pET-ndmA-R2 (see Table S1 in the supplemental material) were used for PCR amplification of *ndmA* from CBB5 genomic DNA using *Pfu*Ultra DNA polymerase with a thermal profile of 30 s at 95°C, 30 s at 58°C, and 60 s at 72°C for 30 cycles. The PCR product was digested with NdeI and EcoRI and then ligated into the plasmid pET32a previously digested with NdeI and EcoRI, producing plasmid pET-ndmA. A site-directed mutagenesis procedure was carried out using the procedure described in the QuikChange II site-directed mutagenesis kit (Stratagene) to remove the *ndmA* stop codon and fuse the His_6 tag on pET32a to the 3′ end of *ndmA*. PCR primers ndmA-Histag-F and ndmA-Histag-R (see Table S1) were used in this site-directed mutagenesis procedure, and the resultant plasmid was designated pET-ndmA-His.

ndmB was cloned into pET32a as a C-terminal His tag fusion gene using the overlap extension PCR procedure described by Bryksin and Matsumura (6). Chimeric primers OE_PCR-F2 and OE_PCR-R (see Table S1 in the supplemental material) were used in a PCR to amplify *ndmB* from CBB5 genomic DNA using *Taq* DNA polymerase, with a thermal profile of 30 s at 94°C, 30 s at 60°C, and 45 s at 72°C for 30 cycles. The 1.1-kb PCR product was gel purified and used as a mega-primer in a second round of PCR with 3 ng of pET32a as the template and Phusion HF DNA polymerase. The thermal profile was 10 s at 98°C, 30 s at 60°C, and 3.5 min at 72°C for 20 cycles. After completion of PCR, 20 units of DpnI was directly added to the PCR and the mixture was incubated at 37°C for 1 h. The reaction was then electroporated into electrocompetent E. cloni 10G cells (Lucigen, Middleton, WI), and plasmid pET32-ndmB-His was recovered.

Forward primer ndmD-F-NdeI and reverse primer ndmD-R-HindIII (see Table S1 in the supplemental material) were designed to amplify *ndmD* from CBB5 genomic DNA using *Taq* DNA polymerase with a thermal profile of 30 s at 95°C, 30 s at 55°C, and 90 s at 72°C for five cycles, followed by 30 s at 95°C, 30 s at 60°C, and 90 s at 72°C for 30 cycles. The PCR product was cloned into the pGEM-T Easy vector, resulting in plasmid pTA-ndmD. The cloned *ndmD* was then released from pTA-ndmD by digestion with NdeI plus EcoRI and ligated to pET28a which was previously digested with NdeI and EcoRI, resulting in plasmid pET28-His-ndmD.

DNA sequencing of pET28-ndmA-His, pET28-ndmB-His, and pET28-His-ndmD confirmed that PCR amplification did not introduce any mutations into *ndmA*, *ndmB*, or *ndmD*.

Plasmids pET32-ndmA-His, pET32-ndmB-His, and pET28-His-ndmD were individually transformed into *E. coli* BL21(DE3) for overproduction of recombinant proteins. Expression of *ndmA*-His and *ndmB*-His was carried out in the same manner. The cells were grown in LB broth with 100 $\mu g \cdot ml^{-1}$ ampicillin at 37°C with agitation at 250 rpm. When the cell density reached an optical density at 600 nm (OD_{600}) of 0.5, sterile iron (III) chloride was added to the culture at a final concentration of 10 μM, and the culture was shifted to 18°C for incubation. IPTG at a final concentration of 0.1 mM (for *ndmA*) or 1 mM (for *ndmB*) was added to induce gene expression when the OD_{600} reached 0.8 to 1.0. Induced cells were incubated at 18°C for 18 h and harvested by centrifugation. Cells were stored at −80°C prior to lysis.

Expression of His-*ndmD* was carried out in a similar manner, with minor modifications. Cells were grown in Terrific broth with 30 $\mu g \cdot ml^{-1}$ kanamycin at 37°C with agitation at 250 rpm. When the cell density reached an OD_{600} of 0.5, sterile $FeCl_3$ and ethanol were added to the culture at final concentrations of 10 μM and 0.1% (vol/vol), respectively, and the culture was shifted to incubation at 18°C. When the OD_{600} of the culture reached 0.8, IPTG was added to a final concentration of 0.2 mM. The culture was incubated at 18°C for 18 h and harvested by centrifugation. Cells were stored at −80°C prior to lysis.

Purification of His-tagged NdmA, NdmB, and NdmD. About 5.2 g frozen cells containing NdmA-His_6 and 4.2 g cells containing NdmB-His_6 were thawed and each suspended to a final volume of 30 ml in 25 mM potassium phosphate (KP_i) buffer (pH 7) containing 10 mM imidazole and 300 mM NaCl. Additionally, 40.3 g frozen cells containing His_6-NdmD were suspended to 100 ml in the same buffer. Cells were lysed by passing twice through a chilled French press at 138 MPa. The lysates were centrifuged at 30,000 × *g* for 20 min, and the supernatants were saved as cell extracts for purification of NdmA-His_6, NdmB-His_6, and His_6-NdmD.

All enzyme purification was performed at 4°C using an automated fast protein liquid chromatography system (ÄKTA FPLC system; Amersham Pharmacia Biotech). Cell extracts containing soluble enzyme were purified on a 40-ml (bed volume) Ni-NTA column (GE Healthcare) at a flow rate of 5 $ml \cdot min^{-1}$. The column was preequilibrated in binding buffer consisting of 300 mM NaCl and 10 mM imidazole in 25 mM KP_i buffer (pH 7). Thirty milliliters of cell extract containing NdmA-His_6 or NdmB-His_6 and 80 ml cell extract containing His_6-NdmD were passed through the Ni-NTA column to allow for binding of His-tagged proteins. Unbound protein was washed from the column with 200 ml binding buffer. Bound protein was then eluted with 120 ml elution buffer consisting of 300 mM NaCl and 250 mM imidazole in 25 mM KP_i buffer (pH 7) and concentrated using Amicon ultrafiltration units (molecular weight cutoff [MWCO], 30,000). Each concentrated enzyme solution was dialyzed (MWCO, 10,000) at 4°C against 2 litres of 50 mM KP_i buffer (pH 7.5) with 5% (vol/vol) glycerol and 1 mM dithiothreitol (DTT) (KPGD buffer) with four changes of dialysis buffer within 24 h to remove imidazole. All purified enzymes were stored short-term on ice and at −80°C for long-term storage.

Preparation of NdmC-enriched fraction. *P. putida* CBB5 was grown in M9 mineral salts medium (26) supplemented with 0.4% Soytone and 0.25% caffeine at 30°C with 250-rpm rotary shaking. About 12.5 g (wet weight) CBB5 was suspended in 25 ml 50 mM KP_i buffer (pH 7.5) with 10 $\mu g \cdot ml^{-1}$ DNase I. Cells were broken using a French press as described above. Unbroken cells and debris were removed from the lysate by centrifugation (16,000 × *g* for 10 min at 4°C), and the supernatant was designated the cell extract.

The partially purified fraction containing NdmC and NdmD activity (previously designated Ccr) was prepared by separation on DEAE Sepharose and phenyl Sepharose as described previously (30). The Ccr fraction, which eluted from phenyl Sepharose under 0.25 to 0 M ammonium sulfate, was washed twice with 60 ml 50 mM KPGD buffer and concentrated to 1 ml using Amicon ultrafiltration units with an MWCO of 10,000. This concentrated Ccr fraction was loaded onto a 5-ml Q Sepharose column (GE Healthcare) preequilibrated in KPGD buffer. After unbound proteins were washed from the column with 15 ml equilibration buffer, bound proteins were eluted with a 15-ml linear gradient of KCl (0 to 0.1 M) followed by a 180-ml linear gradient of KCl (0.1 to 0.4 M) in KPGD buffer. NdmC and NdmD activities coeluted from the Q Sepharose column and were concentrated to 2 ml using Amicon 10,000-MWCO ultrafiltration units.

The Q Sepharose-purified fraction was washed three times with 30 ml 5 mM KPGD buffer (pH 6.0) and loaded onto a 15-ml hydroxyapatite column (Bio-Rad). The unbound protein was washed from the column with 15 ml equilibration buffer, and bound protein was eluted from the column with a 180-ml linear gradient of KPGD buffer (5 to 250 mM). The NdmC and NdmD activities coeluted under 200 mM KPGD buffer and were concentrated to 1 ml with Amicon 10,000-MWCO ultrafiltration units.

Molecular masses of purified proteins were estimated under denaturing conditions by PAGE on 10% Bis-Tris gels with MOPS (morpholinepropanesulfonic acid) running buffer (Invitrogen). Gels were stained for viewing with GelCode blue safe protein stain (Thermo Fisher Scientific, Waltham, MA).

Enzyme activity assays. NADH:cytochrome *c* oxidoreductase activity was determined as described by Ueda et al. (32). A typical 1-ml reaction in 50 mM KP_i buffer (pH 7.5) contained 300 μM NADH, 87 μM bovine cytochrome *c* (type III; Sigma), and 1.8 μg of partially purified reductase from CBB5 or 0.2 μg of purified His_6-NdmD. The activity was determined by monitoring the increase in absorbance at 550 nm due to reduction of cytochrome *c* at 30°C. An extinction coefficient of 21,000 M^{-1} cm^{-1} for reduced minus oxidized cytochrome *c* was used for quantitating the activity. One unit of activity was defined as 1 μmol of cytochrome *c* reduced per min.

Methylxanthine *N*-demethylase activity assay contained, in a 1-ml total volume, 0.5 mM methylxanthine, 0.5 mM NADH, 50 μM $Fe(NH_4)_2(SO_4)_2$, and an appropriate amount of NdmA-His_6 or NdmB-His_6 (7.4 μg to 2.5 mg protein, depending on substrate specificity) in 50 mM KP_i buffer (pH 7.5). Approximately 4 U of partially purified reductase (Ccr), prepared as described previously (30), or 59 U of purified His_6-NdmD was added to the reaction mixture. Catalase from bovine liver (4,000 U) was also added to reaction mixtures containing His_6-NdmD. The reaction mixture was incubated at 30°C with 300-rpm shaking on an incubating microplate shaker (VWR, Radnor, PA). Periodically, a small aliquot was sampled from the reaction mixture and mixed with an equal volume of acetonitrile for quantifying concentrations of methylxanthines and *N*-demethylated products by HPLC. One unit of *N*-demethylase activity was defined as the consumption of 1 μmol methylxanthine per minute.

Determination of kinetic parameters. Apparent kinetic parameters of NdmA-His_6 and NdmB-His_6 were determined by measuring the initial rate of disappearance (v_o) of methylxanthines in 50 mM KP_i buffer (pH 7.5) at 30°C. The initial substrate concentrations ([*S*]) used in these experiments were from 25 to 500 μM. Substrates were incubated with His_6-NdmD plus either NdmA-His_6 or NdmB-His_6 under standard conditions for 15 min as described previously (30).

Determination of oxygen requirement. Oxygen consumption by NdmA-His_6 and NdmB-His_6 during *N*-demethylation of caffeine and theobromine, respectively, were determined in a closed reaction vessel equipped with a Clarke-type oxygen electrode (digital model 10; Rank Brothers Ltd., Cambridge, England). The electrode was calibrated by using glucose oxidase (Sigma) and glucose for consumption of oxygen. An enzyme activity assay was performed at 30°C in a total volume of 1.2 ml of air-saturated 50 mM KP_i buffer (pH 7.5) with about 150 μM caffeine (or theobromine), 200 μM NADH, 50 μM $Fe(NH_4)_2(SO_4)_2$, 4,000 U catalase, 295 μg NdmA-His_6 or 627 μg NdmB-His_6, and 49 U His_6-NdmD. The reaction was initiated by adding NdmA-His_6 (or NdmB-His_6) plus His_6-NdmD after equilibration of all other reaction components for 5 min. After 5.5 min, a 120-μl aliquot was withdrawn from the reaction, immediately mixed with an equal volume of acetonitrile to stop the enzyme reaction, and analyzed for *N*-demethylated product by HPLC. Background oxygen consumption was quantitated in control reaction mixtures containing all reaction components except the methylxanthine substrate.

Formaldehyde determination. Production of formaldehyde during *N*-demethylation of caffeine by NdmA-His_6 and theobromine by NdmB-His_6 was determined by derivatizing formaldehyde with Nash reagent prepared by the method of Jones et al. (18). Standards were prepared with known concentrations of formaldehyde added to control enzyme reaction mixtures without the methylxanthine substrates.

Analytical procedures. Identification and quantification of methylxanthines and their metabolites were conducted with a Shimadzu LC-20AT HPLC system equipped with an SPD-M20A photodiode array detector and a Hypersil BDS C_{18} column (4.6 by 125 mm) as described previously (34). For analysis of 3,5-diacetyl-1,4-dihydrolutidine, methanol-water-acetic acid (30:70:0.5, vol/vol/vol) was used as an isocratic mobile phase at a flow rate of 0.5 ml min^{-1}. For analysis of flavin at 450 nm, 100 μl of His_6-NdmD was added to 900 μl methanol and heated at 95°C for 15 min. The heated mixture was cooled to room temperature, concentrated to 50 μl, and mixed with 50 μl acetonitrile prior to analysis of flavin by HPLC. The retention time of the flavin present in His_6-NdmD was compared to those of standards of flavin adenine dinucleotide (FAD) and flavin mononucleotide (FMN).The protein concentration was determined by the Bradford method (4) using bovine serum albumin as the standard with a dye reagent purchased from Bio-Rad. Iron content in NdmA-His_6 and NdmB-His_6 was determined by inductively coupled plasma mass spectrometry (ICP-MS). An aliquot of purified NdmA-His_6 and NdmB-His_6 was mixed with an equal volume of trace metal-free, ultrapure concentrated nitric acid. The mixture was heated at 160°C for 1 h to break down all organic materials. The acid digest was then diluted appropriately with ultrapure water for quantification of iron by a Thermo X-series II ICP-MS system at the Department of Geosciences, University of Iowa. The ICP-MS system was calibrated with high-purity iron standard solution. Bovine cytochrome *c* was used as a positive control. Acid-labile sulfur content in enzyme was determined colorimetrically using the *N*,*N*-dimethyl-*p*-phenylenediamine assay (29). The N-terminal amino acid sequences of the three major protein bands in the purified protein fraction containing NdmC and NdmD activities were determined at the Protein Facility, Iowa State University, Ames, IA.

Homology modeling. The program MODELLER version 9.10 (25) was used to generate 10 models each of NdmA and NdmB. A ClustalW (21) alignment of NdmA and NdmB with the DdmC (dicamba *O*-demethylase) sequence and the 1.75-Å DdmC structure (Protein Data Bank [PDB] ID 3GKE) (10) as the template was used as the input to MODELLER. The resulting models were superimposed with the 2.1-Å dicamba-bound DdmC structure (PDB ID 3GL2) (10) and analyzed in PyMOL 1.4.1 (Schrödinger, LLC). A caffeine molecule was modeled by hand in the position of the dicamba from 3GL2.

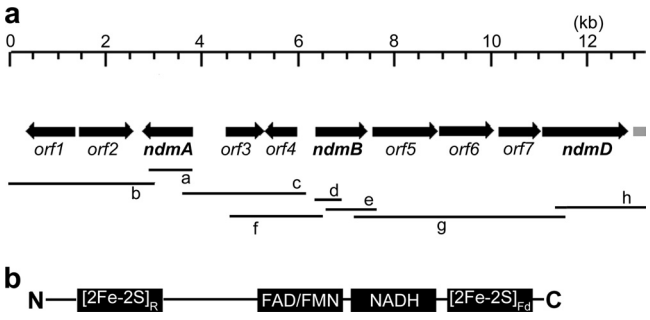

FIG 1 (a) Organization of *ndmABD* and *orf1* to *orf7* in the 13.2-kb gene cluster in *P. putida* CBB5. Black arrows indicate the position and orientation of each *orf*. The gray box directly downstream of *ndmD* represents the 5′ end of a partial ORF, *orf8*. Black lines (labeled a to h) represent the eight overlapping PCR products used to assemble this map. (b) Schematic organization of conserved domains identified in the deduced protein sequence of *ndmD*. Designations: $[2Fe\text{-}2S]_R$, Rieske [2Fe-2S] domain; [FAD/FMN], flavin adenine dinucleotide or flavin mononucleotide binding domain; [NADH], NADH binding domain; $[2Fe\text{-}2S]_{Fd}$, plant-type ferredoxin [2Fe-2S] domain.

Nucleotide sequence accession numbers. The nucleotide sequences of *ndmA* (accession no. JQ061127), *ndmB* (JQ061128), and *ndmD* (JQ061130) have been deposited at the GenBank nucleotide sequence database.

RESULTS

Cloning of an *ndm* gene cluster from CBB5. Degenerate PCR primers were designed from the N-terminal amino acid sequences of NdmA and NdmB (30) and the conserved protein and nucleotide sequences in two hypothetical ROs: *cdm*, a putative caffeine demethylase gene (19), and a hypothetical protein in *Janthinobacterium* sp. Marseille (mma_0224, GenBank accession no. YP_001351914). Using these PCR primers, we amplified two PCR products (fragment a and fragment d, Fig. 1a) from CBB5 genomic DNA, each containing an incomplete open reading frame (ORF), designated *ndmA* and *ndmB,* respectively. In combination with PCR primers designed from the nucleotide sequences of fragments a and d and the plasmid backbone of two size-fractionated genomic libraries of CBB5, we used a nested-PCR approach and successfully amplified DNA regions flanking *ndmA* and *ndmB* (see the supplemental material). Ultimately, eight overlapping PCR products were amplified from the CBB5 genome, covering 13.2 kb of DNA (Fig. 1a). Computational analysis of this genomic region identified 10 complete ORFs, designated *orf1* to *orf7*, *ndmA*, *ndmB*, and *ndmD*, plus the 5′ end of an incomplete ORF designated *orf8* (directly downstream of *ndmD*).

Based on sequence homologies, functions were proposed for *orf1* to *orf7* (Table 1). The theoretical N-terminal protein sequences of *ndmA* and *ndmB* completely matched the N-terminal protein sequences previously obtained from purified NdmA and NdmB proteins. *ndmA* encoded a 40.2-kDa protein consisting of 351 amino acids, consistent with the estimated molecular mass of 40 kDa previously estimated for NdmA by SDS-PAGE. *ndmB* encoded a 40.9-kDa protein with 355 amino acids, which was a larger size than the previously estimated molecular mass of 35 kDa for

TABLE 1 Deduced function of each ORF identified within the 13.2-kb *ndm* gene cluster of *Pseudomonas putida* CBB5

Gene	Size (amino acids)	Database used in BlastP search	Homologous protein	GenBank accession no.	% Identity[a]	Proposed function
orf1	331	NR[b]	*Janthinobacterium* sp. Marseille mma_0222	YP_001351912	48	AraC family transcription regulator
		SwissProt	*Sinorhizobium meliloti* GlxA	O87389	20	
orf2	370	NR	*Pseudomonas mendocina* NK-01 MDS_2843	YP_004380626	90	Glutathione-dependent formaldehyde dehydrogenase
		SwissProt	*Synechocystis* sp. PCC 6803 FrmA	NP_440484	72	
orf3	263	NR	*P. putida* TJI-51 G1E_06918	EGB99698	53	Putative outer membrane protein
		SwissProt	*Vibrio parahaemolyticus* OmpK	P51002	18	
orf4	220	NR	*Janthinobacterium* sp. Marseille mma_3679	YP_001355369	63	GntR family transcriptional regulator
		SwissProt	*Bacillus subtilis* YdhC	O05494	21	
orf5	447	NR	*Janthinobacterium* sp. Marseille mma_PbuX7	YP_001355365	65	Methylxathine transport
		SwissProt	*E. coli* K-12 YgfU	Q46821	51	
orf6	361	NR	*Pseudomonas* sp. TJI-51 G1E_06893	EGB99693	67	Protein with conserved domain belongs to pfam01261; no proposed function in methylxanthine catabolism
		SwissProt	Not found			
orf7	284	NR	*Pseudomonas* sp. TJI-51 G1E_06898	EGB99694	57	Protein with conserved domain belongs to SRPBCC ligand-binding domain superfamily; proposed to encode NdmC, the 7-methylxanthine-specific *N*-demethylase
		SwissProt	*Chlamydomonas reinhardtii* CAO	Q9ZWM5	17	

[a] The percent identity was determined by aligning the gene product of each *orf* with the homologous protein using ClustalW2 (21).
[b] NR, Non-Redundant Protein Sequences Database.

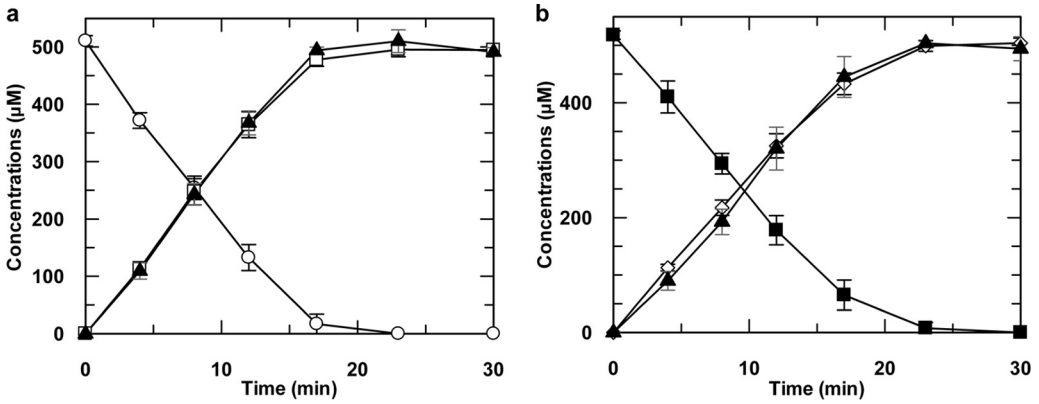

FIG 2 Stoichiometric *N*-demethylation of methylxanthines by NdmA-His_6 and NdmB-His_6. (a) NdmA-His_6 *N*-demethylated 510 ± 10 μM caffeine (○) to 500 ± 10 μM theobromine (□), resulting in production of 510 ± 20 μM formaldehyde (▲), or 1 mol of formaldehyde produced per mol of theobromine formed. (b) NdmB-His_6 *N*-demethylated 510 ± 10 μM theobromine (■) to 500 ± 10 μM 7-methylxanthine (◇) and 500 ± 3 μM formaldehyde (▲). Concentrations reported were means with standard deviations of triplicate results.

purified NdmB by SDS-PAGE (30). Consistent with the SDS-PAGE results, when *ndmB* was expressed as a C-terminal His-tagged protein in *E. coli*, its apparent molecular mass estimated by SDS-PAGE was also smaller than the theoretical MW deduced from the gene sequence (see Fig. S1a in the supplemental material). The protein sequences encoded by *ndmA* and *ndmB* were used as queries for BLASTP search in the GenBank database. Both sequences were homologous to the catalytic α subunits of different ROs. Conserved sequences for a Rieske [2Fe-2S] domain (CX$HX_{16}CX_2H$) and a nonheme Fe(II) domain [(E/D)X_2HX_4H] were identified in the theoretical protein sequences of both *ndmA* and *ndmB*. Furthermore, *ndmA* and *ndmB* transcribed divergently from each other (Fig. 1a), indicating they are not part of the same transcriptional unit. All of these support the hypothesis that NdmA and NdmB could individually function as *N*-demethylating ROs.

A typical reductase gene for ROs was not found directly next to either *ndmA* or *ndmB*. However, *ndmD* was theorized to encode a 65-kDa RO reductase that coupled NADH to *ndmA* and *ndmB*. The NdmD protein sequence had a conserved Rieske-type [2Fe-2S] domain at its N-terminal half (Fig. 1b). Additionally, a flavin-binding domain, an NADH-binding domain, and a plant-type [2Fe-2S] domain were identified at its C-terminal half, similar to FNR_c-type reductases of ROs (20). Some ROs are three-component systems requiring a reductase and a ferredoxin for electron transfer to oxygenase components. In these three-component ROs, the iron-sulfur clusters in the ferredoxins are either the Rieske [2Fe-2S] type or [3Fe-4S] type (20). We hypothesized that *ndmD* represented a unique gene fusion of a ferredoxin gene and a reductase gene into a single ORF and encoded a functional reductase that specifically coupled to NdmA and/or NdmB.

Functional expression and characterization of *ndmA*, *ndmB*, and *ndmD* gene products. *ndmA*, *ndmB*, and *ndmD* were individually expressed as His-tagged fusion proteins in *E. coli* BL21(DE3), and the recombinant proteins were purified using nickel-affinity chromatography (see Fig. S2a in the supplemental material). Purified His_6-NdmD contained four atoms of iron, four acid-labile sulfur atoms, and one molecule of FMN per His_6-NdmD monomer. The flavin prosthetic group in His_6-NdmD was released by boiling, indicating that it is not covalently bound. The iron, acid-labile sulfur, and flavin content in His_6-NdmD were in agreement with the presence of a Rieske [2Fe-2S] domain, a plant-type [2Fe-2S] domain, and a flavin-binding domain predicted by the *ndmD* gene sequence. His_6-NdmD oxidized NADH and reduced cytochrome *c* concomitantly, similar to several RO reductases (15, 28, 33). However, His_6-NdmD could not *N*-demethylate caffeine or any related methylxanthine in the presence or absence of NADH and Fe^{2+}.

Purified NdmA-His_6 and NdmB-His_6 (see Fig. S2a in the supplemental material) each contained approximately 2 mol of acid-labile sulfur and 2 mol of iron per mol of enzyme monomer. The iron content is lower than the expected value of 3 Fe per α subunit for ROs, which is probably due to dissociation of nonheme Fe from proteins during purification. UV/visible absorption spectra of oxidized NdmA-His_6 and NdmB-His_6 (see Fig. S2b and c in the supplemental material) are similar to those of other well-characterized ROs, with absorption maxima at 319, 453, and 553 nm and 320, 434, and 550 nm, respectively. Purified NdmA-His_6 and NdmB-His_6 could neither oxidize NADH nor reduce cytochrome *c*. Additionally, neither of them could *N*-demethylate caffeine or any related methylxanthine in the presence or absence of NADH and Fe^{2+}. However, when NdmA-His_6 was incubated with His_6-NdmD, caffeine, NADH, and exogenous Fe^{2+}, caffeine was stoichiometrically N_1-demethylated to theobromine (3,7-dimethylxanthine) and formaldehyde (Fig. 2a). Incubation of NdmB-His_6 with His_6-NdmD, theobromine, NADH, and Fe^{2+} resulted in stoichiometric N_3-demethylation of theobromine to 7-methylxanthine and formaldehyde (Fig. 2b). One O_2 is consumed for the removal of each *N*-methyl group from the methylxanthine substrates by either NdmA-His_6 or NdmB-His_6 (Fig. 3).

The functions of NdmA and NdmB as position-specific methylxanthine *N*-demethylases were further supported by the steady-state kinetic parameters of these two enzymes (Table 2). Theobromine was the preferred substrate for NdmB-His_6, with the highest k_{cat}/K_m value of 1.8 ± 0.4 min^{-1} μM^{-1}, followed closely by 3-methylxanthine. The catalytic efficiencies of NdmB-His_6 for methylxanthines containing an N_1-methyl group were 10^2 to 10^3 times lower than those of theobromine or 3-methylxanthine. NdmB-His_6 had no activity on paraxanthine, 1-methylxanthine, or 7-methylxanthine. Clearly, NdmB-His_6 was highly specific for

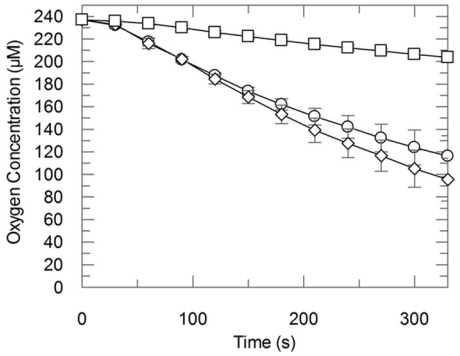

FIG 3 Consumption of O_2 by NdmA-His_6 and NdmB-His_6 during *N*-demethylation of caffeine and theobromine, respectively. *N*-Demethylation of 150 ± 3 μM caffeine to 140 ± 3 μM theobromine by NdmA-His_6 with consumption of 130 ± 20 μM O_2 (○) and of 140 ± 20 μM theobromine to 140 ± 9 μM 7-methylxanthine by NdmB-His_6 with consumption of 130 ± 10 μM O_2 (◇) is shown. Background oxygen consumption in an enzyme reaction with either NdmA-His_6 or NdmB-His_6 but without methylxanthine is also shown (□). Concentrations reported were means with standard deviations of triplicate results.

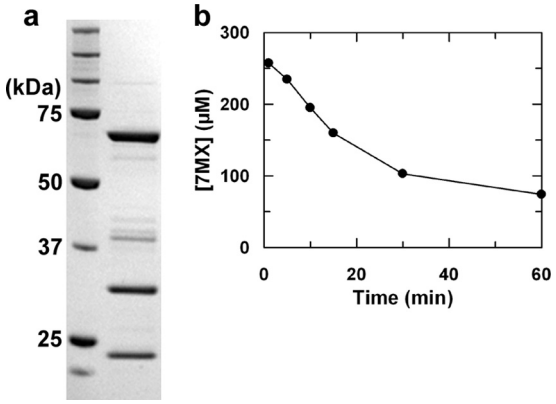

FIG 4 An SDS-PAGE gel (a) and N_7-demethylation of 7-methylxanthine (b) by a highly enriched enzyme preparation containing NdmC and NdmD activities. Three major protein bands with estimated molecular masses of 67, 32, and 22 kDa were present in this highly enriched enzyme preparation.

N_3-linked methyl groups of methylxanthines. In contrast, theophylline was the preferred substrate for NdmA-His_6, followed by caffeine and paraxanthine. NdmA-His_6 had low activity on 1-methylxanthine and was inactive on theobromine, 3-methylxanthine, and 7-methylxanthine. Thus, NdmA-His_6 catalyzed the demethylation only at the N_1 position of methylxanthines. Various methylated purine and pyrimidine analogs were not *N*-demethylated by NdmA-His_6 and NdmB-His_6, suggesting that both enzymes are unlikely to be broad-specificity purine demethylases involved in nucleic acid repair (1).

Identification of NdmC, a 7-methylxanthine-specific *N*-demethylase, in CBB5. Previously, when purified Ndm (containing both NdmA and NdmB) was coupled with a partially purified reductase fraction (designated Ccr) from CBB5, caffeine was completely *N*-demethylated to xanthine (30). This result indicated the presence of an N_7-demethylase activity in CBB5, which was not associated with NdmA, NdmB, or NdmD. We have now confirmed that this N_7-demethylase activity, designated NdmC, was copurifying with NdmD in previous experiments. As shown in Fig. 4a, a highly enriched protein fraction with NdmC activity contained 3 major protein bands when analyzed by SDS-PAGE. N-terminal protein sequences were determined for all three bands. The N-terminal protein sequence of the 67-kDa band was identical to the *ndmD* gene product. Furthermore, the N-terminal protein sequences of the 32-kDa and 22-kDa bands were identical to those encoded by *orf7* and the incomplete ORF *orf8*, respectively. This highly enriched NdmC fraction specifically N_7-demethylated 7-methylxanthine to xanthine at the same rates observed in reaction mixtures containing active NdmA-His_6 or NdmB-His_6 (Fig. 4b). Caffeine, paraxanthine, and theobromine were not *N*-demethylated by this fraction, indicating that 7-methylxanthine was the sole substrate for NdmC.

TABLE 2 Kinetic parameters of NdmA and NdmB

Enzyme	Substrate[a]	Product	K_m (μM)[b]	k_{cat} (min^{-1})[b]	k_{cat}/K_m ($min^{-1} \cdot \mu M^{-1}$)
NdmA-His_6	Caffeine	Theobromine	37 ± 8	190 ± 10	5.1 ± 1.2
	Theophylline	3-Methylxanthine	9.1 ± 1.7	83 ± 1.7	9.1 ± 1.7
	Paraxanthine	7-Methylxanthine	53 ± 20	130 ± 10	2.5 ± 0.8
	Theobromine		>500	NA[c]	NA
	1-Methylxanthine	Xanthine	270 ± 50	16 ± 1	0.06 ± 0.01
	3-Methylxanthine		>500	NA	NA
	7-Methylxanthine		>500	NA	NA
NdmB-His_6	Caffeine	Paraxanthine	42 ± 9	0.23 ± 0.03	0.006 ± 0.001
	Theophylline	1-Methylxanthine	170 ± 50	0.27 ± 0.03	0.016 ± 0.005
	Paraxanthine		>500	NA	NA
	Theobromine	7-Methylxanthine	25 ± 5	46 ± 1.9	1.8 ± 0.4
	1-Methylxanthine		>500	NA	NA
	3-Methylxanthine	Xanthine	22 ± 5	32 ± 1.5	1.4 ± 0.3
	7-Methylxanthine		>500	NA	NA

[a] The following purine and pyrimidine analogs were tested as substrates for NdmA-His_6 and NdmB-His_6 but had no activity: 1-methylguanine, 1-methyladenine, 3-methyladenine, 1,3-diemethyluracil.
[b] Average and standard deviation were derived from three independent assays. Initial reaction rates were determined by following substrate disappearance using HPLC.
[c] NA, no activity.

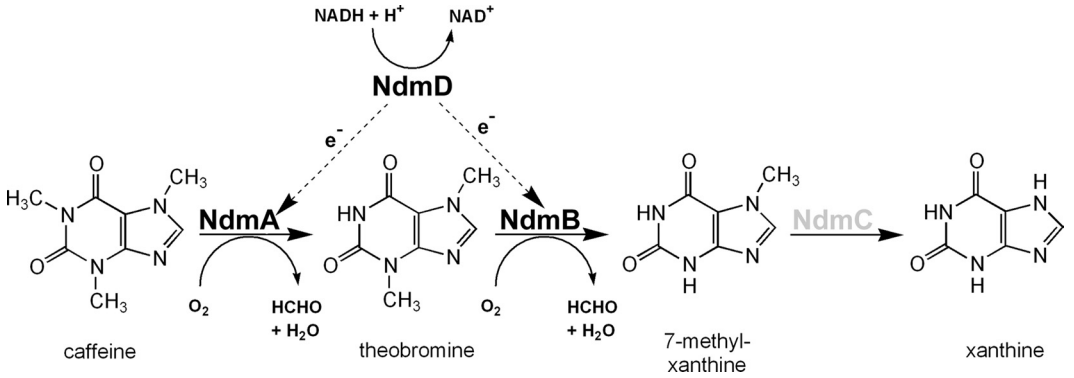

FIG 5 Proposed sequential *N*-demethylation of caffeine by *Pseudomonas putida* CBB5, based on catalytic efficiencies of NdmA-His$_6$ and NdmB-His$_6$. *N*-Demethylation of caffeine is initiated at the N_1 position by NdmA, forming theobromine. NdmB then catalyzes removal of the *N*-linked methyl group at the N_3 position, producing 7-methylxanthine. Oxygen is the cosubstrate for NdmA and NdmB. NdmD couples with NdmA and NdmB by transferring electrons from NADH to NdmA and NdmB for oxygen activation. Each methyl group removed results in the formation of one formaldehyde. NdmC is proposed to be specific for *N*-demethylation of 7-methylxanthine to xanthine.

DISCUSSION

In this report, we have identified and characterized the genes of *P. putida* CBB5 responsible for *N*-demethylation of caffeine and related methylxanthines, which is the essential first step for assimilating the carbon and nitrogen in caffeine. *ndmA* and *ndmB*, respectively, encode N_1- and N_3-specific methylxanthine demethylases (Table 2), allowing caffeine to be metabolized to 7-methylxanthine. The consumption of one O_2 by either NdmA or NdmB to remove one *N*-linked methyl group from methylxanthines as formaldehyde suggests that NdmA and NdmB are monooxygenases. NdmA and NdmB activities are dependent on a reductase component, which is encoded by *ndmD*, as illustrated in this report. NdmD oxidizes NADH and transfers electrons to NdmA and NdmB, which catalyze the *N*-demethylation reactions.

Previously, we purified a methylxanthine *N*-demethylase, Ndm, from *P. putida* CBB5. Ndm was composed of both NdmA and NdmB, which were not separable by several chromatographic steps (30). Therefore, we concluded that NdmA and NdmB were two subunits of a single broad-specificity *N*-demethylase, Ndm. In this report, conclusive evidence has been provided that NdmA and NdmB are individual *N*-demethylases with unique substrate specificities. The physical properties (shape, surface charge density, MW, etc.) of NdmA and NdmB appear to be very similar, resulting in their previous copurification. Based on the substrate specificities of NdmA and NdmB, we propose that the *N*-demethylation of caffeine by CBB5 occurs primarily in the sequence depicted in Fig. 5. The N_1-methyl group is first removed from caffeine by NdmA, forming theobromine, which is the preferred substrate of NdmB. NdmB then removes the N_3-methyl group, producing 7-methylxanthine.

The gene sequences of *ndmA* and *ndmB* support our previous hypothesis of Ndm as an RO. Conserved sequences for a Rieske [2Fe-2S] domain and a mononuclear nonheme Fe(II) domain, which is most likely the site of oxidation, are identified in the protein sequences deduced from *ndmA* and *ndmB*. The dependency of NdmA and NdmB on the reductase component (NdmD), UV/visible absorption spectra, utilization of oxygen as a cosubstrate, and stimulation of NdmA and NdmB activity by exogenous Fe^{2+} are characteristics commonly found among ROs. Traditionally, ROs have been classified according to their electron transport components (3). However, Gibson and Parales (13) have demonstrated in a phylogenetic analysis that the catalytic α subunit of ROs clustered into four major groups according to the substrates utilized by the ROs. We extended this analysis and constructed a rootless phylogenetic tree including NdmA and NdmB, plus 64 well-characterized ROs (see Fig. S2 in the supplemental material).

NdmA and NdmB clustered with Cdm and the hypothetical RO in *Janthinobacterium* sp. Marseille (mma_0224) in a distinct clade. Cdm, being 89% identical to NdmA, is likely to be a caffeine *N*-demethylase. The function of mma_0224 is not clear, as it is 53% and 58% identical to NdmA and NdmB, respectively. The nearest-neighbor clades to NdmA and NdmB contain ROs that catalyze *O*-demethylation or cleavage of C-N or C-O bonds. Some of them are monooxygenases (e.g., DdmC and VanA), while others are dioxygenases (such as CarAa). The homology between these enzymes and either NdmA (9 to 17% identity) or NdmB (8 to 15% identity) is minimal and restricted to the N-terminal regions of these proteins where the Rieske [2Fe-2S] domain is located. The low degree of similarity between NdmA/NdmB and other ROs is not surprising considering the diversity of specific substrates used by these enzymes and the fact that the specific substrate binding site of ROs is predominantly at the C-terminal portion of RO α subunits (11). Our phylogenetic analysis did not support monophylogeny between NdmA/NdmB with the majority of ROs, which hydroxylate aromatic ring substrates. It is likely that divergent evolution of ROs resulted in two groups, one for catalyzing aromatic ring hydroxylations and one for C-O/C-N bond-cleaving reactions.

When Ndm was purified previously from *P. putida* CBB5, Ndm activity was assayed using a partially purified reductase component isolated from CBB5 (30). Under that assay condition, we observed complete *N*-demethylation of caffeine to xanthine. NdmA and NdmB present in Ndm accounted for the N_1- and N_3-demethylation activities, respectively. However, neither NdmA nor NdmB could be responsible for *N*-demethylation of 7-methylxanthine to xanthine, since 7-methylxanthine is not a substrate for either enzyme (Table 2). Here, we have identified a 7-methylxanthine-specific *N*-demethylation activity, designated NdmC. NdmC was found to copurify with NdmD (Fig. 4a). The highly

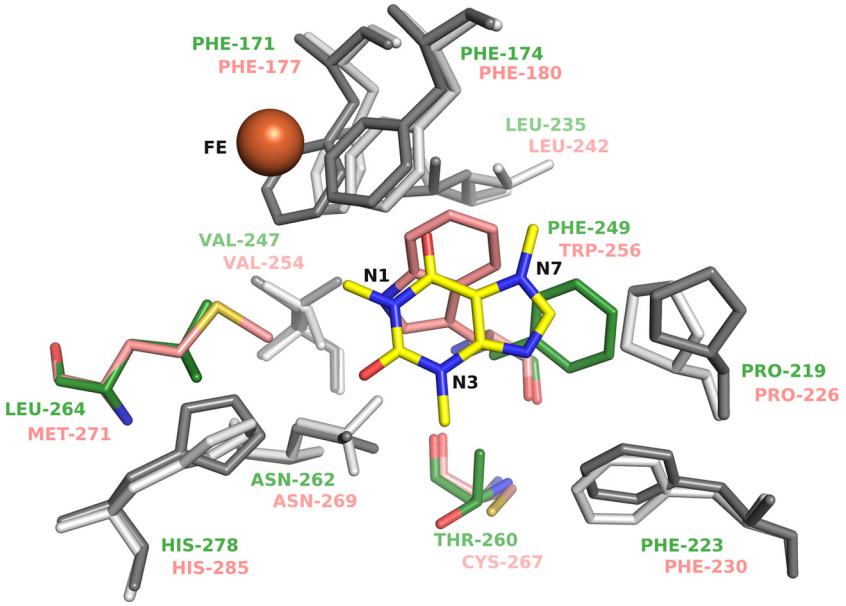

FIG 6 Active site model of NdmA and NdmB, Residues lining the active site cavities of NdmA and NdmB homology models are shown as sticks. Residues conserved between NdmA and NdmB are colored light gray and dark gray, respectively. Nonconserved residues are colored green (NdmA) and salmon (NdmB). Caffeine (yellow sticks) is modeled into the active site at the position of dicamba in DdmC (PDB ID 3GL2) (10). The nonheme iron from the dicamba structure is shown as an orange sphere.

enriched reductase fraction contained NdmD plus two additional major protein bands. From their respective N-terminal protein sequences, the genes encoding these two proteins were identified as *orf7* and *orf8* in the *ndm* gene cluster (Fig. 1a). Although *orf8* is an incomplete ORF, its partial theoretical protein sequence displayed significant similarity to various glutathione-*S*-transferases. Meanwhile, the theoretical protein sequence deduced from *orf7* showed its significant identity to proteins with a conserved domain belonging to the SRPBCC ligand-binding domain superfamily. Included in this superfamily are the C-terminal catalytic domains of aromatic ring-hydroxylating RO α subunits. Interestingly, a conserved sequence of a Rieske [2Fe-2S] domain was not present in the deduced protein sequence of *orf7*. However, a conserved sequence of a mononuclear nonheme Fe(II) domain, which is usually the catalytic site for ROs, was identified in *orf7*. We currently hypothesize that *orf7* encodes NdmC, the *N*-demethylase specific for 7-methylxanthine. Expression of this protein to confirm N_7-demethylase activity has proven difficult due to formation of inclusion bodies under various cloning and growth conditions.

DdmC (dicamba *O*-demethylase) is one of the few ROs with available crystal structures (10) (PDB ID 3GKE) that are evolutionarily related to NdmA and NdmB, and it was also the top match in a BLAST search against the PDB for NdmA and NdmB sequences. NdmA and NdmB share only about 40% similarity (~20% identity) with DdmC across approximately 350 residues. Therefore, NdmA and NdmB homology models were generated using DdmC as a structural template (Fig. 6). A comparison of the active sites in the NdmA and NdmB homology models indicates that the pocket can readily accommodate caffeine next to the nonheme iron for demethylation. Most of the residues lining the active site pocket in NdmA and NdmB superimpose very well across the 10 models generated for each (Fig. 6). There are only three residues in the binding pocket that are not conserved between NdmA (Phe249, Thr260, and Leu264) and NdmB (Trp256, Cys267, and Met271). The most notable nonconserved pair is Phe249 in NdmA and Trp256 in NdmB. Both residues are close to the catalytic nonheme iron. Trp256 was found to explore multiple conformations in the various homology models generated, all of which altered the shape of the cavity near the catalytic site significantly. It seems that steric effects due to the shape and size of the residue at this position in NdmA and NdmB may be one of the contributing factors that alter the binding orientation of the ligand affecting substrate specificity. Similar effects of bound ligand orientation on substrate specificity and product selectivity have been previously discussed for ROs (11). Any further structural features that explain the specificity difference between NdmA and NdmB must await crystal structure elucidation, which is in progress.

In summary, we propose that utilization of caffeine by CBB5 occurs via *N*-demethylation in a preferential, ordered sequence (Fig. 5). This ordered *N*-demethylation of caffeine is catalyzed by NdmA and NdmB at the N_1 and N_3 positions, respectively, of various methylxanthines. Both NdmA and NdmB are monooxygenases; one O_2 is consumed per *N*-methyl group removed as formaldehyde. NdmD appears to be the sole reductase for transfer of electrons from NADH to NdmA, NdmB, and possibly NdmC, for oxygen activation and *N*-demethylation to formaldehyde. Although we have established enzymologically that NdmC catalyzes N_7-demethylation of 7-methylxanthine, the gene correlation has not yet been established. This discovery of highly specific methylxanthine *N*-demethylases has shed light on the long-standing question of how bacteria are able to use caffeine and other methylxanthines as sole carbon and nitrogen sources. CBB5 is able to use xanthine, formaldehyde, and formate, which are liberated

from caffeine and other methylxanthines, for growth (data not shown).

NdmA, NdmB, and NdmC could have broad applications in bioremediation of environments contaminated by caffeine and related methylxanthines, particularly in countries with large coffee- and tea-processing industries. These genes could also find utility in detecting caffeine, a marker for human activities, in wastewater streams (7), or in converting the enormous waste generated via manufacturing of coffee and tea to animal feed and feedstocks for fuels and fine chemicals (24). Last, but not least, these genes could prove useful in the production of pharmaceutically useful modified xanthine analogs, which are currently being synthesized by challenging multistep processes (22). The assignment of NdmA and NdmB to the RO enzyme family broadens our understanding of the enzymatic mechanism for *N*-demethylation reactions, as we generally have less knowledge regarding demethylases than methylating enzymes (14). This first report of soluble bacterial RO *N*-demethylases and their complete gene sequences will certainly stimulate the discovery of new *N*-demethylases involved in the degradation of many natural products and xenobiotics.

ACKNOWLEDGMENTS

This research was supported by the University of Iowa Research Funds.

We also thank David Peate and Jay Thompson in the Department of Geoscience for their assistance in the ICP-MS experiment.

REFERENCES

1. **Aas PA, et al.** 2003. Human and bacterial oxidative demethylases repair alkylation damage in both RNA and DNA. Nature **421**:859–863.
2. **Arnaud MJ.** 2011. Pharmacokinetics and metabolism of natural methylxanthines in animal and man, p 33–91. *In* Fredholm BB (ed), Handbook of experimental pharmacology, vol 200. Springer-Verlag, Berlin, Germany.
3. **Batie CJ, Ballou DP, Correll CC.** 1991. Phthalate dioxygenase reductase and related flavin-iron-sulfur containing electron transferases, p 546–566. *In* Müller F (ed), Chemistry and biochemistry of flavoenzymes, vol 3. CRC Press, Boca Raton, FL.
4. **Bradford MM.** 1976. A rapid and sensitive method for the quantitation of microgram quantities of protein utilizing the principle of protein-dye binding. Anal. Biochem. **72**:248–254.
5. **Brunel F, Davidson J.** 1988. Cloning and sequencing of *Pseudomonas* genes encoding vanillate demethylase. J. Bacteriol. **170**:4924–4930.
6. **Bryksin AV, Matsumura I.** 2010. Overlap extension PCR cloning: a simple and reliable way to create recombinant plasmids. Biotechniques **48**: 463–465.
7. **Buerge IJ, Poiger T, Muller MD, Buser HR.** 2006. Combined sewer overflows to surface waters detected by the anthropogenic marker caffeine. Environ. Sci. Technol. **40**:4096–4102.
8. **Dash SS, Gummadi SN.** 2006. Catabolic pathways and biotechnological applications of microbial caffeine degradation. Biotechnol. Lett. **28**:1993–2002.
9. **Delcher AL, Harmon D, Kasif S, White O, Salzberg SL.** 1999. Improved microbial gene identification with GLIMMER. Nucleic Acids Res. **27**: 4636–4641.
10. **Dumitru R, Wang WZ, Weeks DP, Wilson MA.** 2009. Crystal structure of dicamba monooxygenase: a Rieske nonheme oxygenase that catalyzes oxidative demethylation. J. Mol. Biol. **392**:498–510.
11. **Ferraro DJ, Gakhar L, Ramaswamy S.** 2005. Rieske business: structure-function of Rieske non-heme oxygenases. Biochem. Biophys. Res. Commun. **338**:175–190.
12. **Gerken T, et al.** 2007. The obesity-associated FTO gene encodes a 2-oxoglutarate-dependent nucleic acid demethylase. Science **318**:1469–1472.
13. **Gibson DT, Parales RE.** 2000. Aromatic hydrocarbon dioxygenases in environmental biotechnology. Curr. Opin. Biotechnol. **11**:236–243.
14. **Hagel JM, Facchini PJ.** 2010. Biochemistry and occurrence of *O*-demethylation in plant metabolism. Front. Physiol. **1**:14.
15. **Haigler BE, Gibson DT.** 1990. Purifcation and properties of NADH-ferredoxin$_{NAP}$ reductase, a component of naphthalene dioxygenase from *Pseudomonas* sp. strain NCIB 9816. J. Bacteriol. **172**:457–464.
16. **Herman PL, et al.** 2005. A three-component dicamba *O*-demethylase from *Pseudomonas maltophilia*, strain DI-6: gene isolation, characterization, and heterologous expression. J. Biol. Chem. **280**:24759–24767.
17. **Hollenberg PF.** 1992. Mechanisms of cytochrome P450 and peroxidase-catalyzed xenobiotic metabolism. FASEB J. **6**:686–694.
18. **Jones SB, Terry CM, Lister TE, Johnson DC.** 1999. Determination of submicromolar concentrations of formaldehyde by liquid chromatography. Anal. Chem. **71**:4030–4033.
19. **Koide Y, Nakane S, Imai Y.** August 1996. Caffeine demethylate gene-containing DNA fragment and microbial process for producing 3-methyl-7-alkylxanthine. US patent US5550041.
20. **Kweon O, et al.** 2008. A new classification system for bacterial Rieske non-heme iron aromatic ring-hydroxylating oxygenases. BMC Biochem. **9**:11.
21. **Larkin MA, et al.** 2007. Clustal W and Clustal X version 2.0. Bioinformatics **23**:2947–2948.
22. **Liu G, Reddy PSMM, Barber JR, Ng SC, Zhou YF.** 2010. Synthesis of novel 3,7-dihydro-purine-2,6-dione derivatives. Synthetic Commun. **40**: 1418–1436.
23. **Lukashin AV, Borodovsky M.** 1998. GeneMark.hmm: new solutions for gene finding. Nucleic Acids Res. **26**:1107–1115.
24. **Mussatto SI, Machado EMS, Martins S, Teixeira JA.** 2011. Production, composition, and application of coffee and its industrial residues. Food Bioprocess. Tech. **4**:661–672.
25. **Sali A, Blundell TL.** 1993. Comparative protein modelling by satisfaction of spatial restraints. J. Mol. Biol. **234**:779–815.
26. **Sambrook J, Fritsch EF, Maniatis T.** 1989. Molecular cloning: a laboratory manual, 2nd ed. Cold Spring Harbor Laboratory Press, Cold Spring Harbor, NY.
27. **Shi Y, et al.** 2004. Histone demethylation mediated by the nuclear amine oxidase homolog LSD1. Cell **119**:941–953.
28. **Subramanian V, Liu T, Yeh W, Gibson DT.** 1979. Toluene dioxygenase: purification of an iron-sulfur protein by affinity chromatography. Biochem. Biophys. Res. Commun. **91**:1131–1139.
29. **Suhara K, Takemori S, Katagiri M, Wada K, Kobayashi H.** 1975. Estimation of labile sulfide in iron-sulfur proteins. Anal. Biochem. **68**: 632–636.
30. **Summers RM, Louie TM, Yu CL, Subramanian M.** 2011. Characterization of a broad-specificity non-haem iron *N*-demethylase from *Pseudomonas putida* CBB5 capable of utilizing several purine alkaloids as sole carbon and nitrogen source. Microbiology **157**:583–592.
31. **Tsukada Y, et al.** 2006. Histone demethylation by a family of JmjC domain-containing proteins. Nature **439**:811–816.
32. **Ueda T, Lode ET, Coon MJ.** 1972. Enzymatic ω-oxidation. VI. Isolation of homogenous reduced diphosphopyridine nucleotide-rubredoxin reductase. J. Biol. Chem. **247**:2109–2116.
33. **Yu CL, et al.** 2007. Purification, characterization, and crystallization of the components of a biphenyl dioxygenase system from *Sphingobium yanoikuyae* B1. J. Ind. Microbiol. Biotechnol. **34**:311–324.
34. **Yu CL, et al.** 2009. Two distinct pathways for metabolism of theophylline and caffeine are coexpressed in *Pseudomonas putida* CBB5. J. Bacteriol. **191**:4624–4632.